Published by Avanti Publishers

Global Journal of Energy Technology Research Updates

ISSN (online): 2409-5818

Thermodynamic and Exergetic Analysis of the Allam Cycle

Elisa Mariani*, Lorenzo Talluri and Giampaolo Manfrida

University of Florence, Italy

ARTICLE INFO

Article Type: Research Article

Keywords:
Allam cycle
Zero-emission
Carbon dioxide
Oxy-combustion
Decarbonisation

Timeline:
Received: August 29, 2021
Accepted: October 25, 2021
Published December 28, 2021

Citation: Mariani E, Talluri L, Manfrida G. Thermodynamic and Exergetic Analysis of the Allam Cycle. Glob J Energ Technol Res Updat. 2021; 8: 19-34.

DOI: https://doi.org/10.15377/2409-5818.2021.08.2

ABSTRACT

This paper presents the study on the current developments of oxy-combustion thermodynamic cycles, which use the CO2 produced by combustion within the cycle itself without releases into the atmosphere. This is the cause of the attention paid to this type of technology and which makes these cycles one of the avant-gardes of power plants. In particular, this study focuses on the analysis of the Allam cycle with the aim of evaluating its performance and therefore investigating whether it may be an alternative to the series of CO2 control technologies. In this paper, a first principle efficiency of 54.6% and a second principle efficiency of 55.7% are estimated, confirming the outstanding prospect of the NET Power cycle.

*Corresponding Author
Email: e.mariani_1997@libero.it
Tel: +39 3341095723

1. Introduction

The carbon dioxide (CO_2) produced by the combustion of fossil fuels is an important contributor to the greenhouse effect. Therefore, decarbonisation is the simplest way to reduce carbon emissions in the coming years and is considered one of the most promising technologies for tackling CO_2 emissions from fossil fuel-fired power plants. With nearly zero-emission power plants, you can have control over CO_2 released into the atmosphere, while continuing to burn fossil fuels. This is possible using cycles that have carbon dioxide itself as a working fluid.

The fuel considered in this analysis is methane and the oxidant is 99.5% purity oxygen, produced in an Air Separation Unit (ASU). Consequently, the combustion reaction is expressed by equation 1.

$$CH_4 + 2O_2 \rightarrow CO_2 + 2H_2O \quad (1)$$

The fuel is burned in the oxygen produced by the air separation unit (ASU) and the resulting fumes consist mainly of CO_2 and water. Then CO_2 can be easily separated from water by removing the latter by condensation. The oxy-fuel system that uses gaseous fuel (as natural gas) and high purity oxygen is also called the “oxyturbine” system. A variety of such systems have been proposed in recent decades including the Matiant cycle and the Allam cycle. The new CO_2 is captured and sent into the cycle as a working fluid, nothing is released into the atmosphere: a zero-emission system is created.

Regarding the water and CO_2 produced by combustion, the first is removed by condensation, regarding the second one, since it is introduced into the power cycle, a part of it must be constantly removed from the process. The purge stream contains approximately 97% CO_2 and can be used in other applications [5].

Furthermore, if water-based cycles have as a disadvantage the loss of exergy during evaporation and condensation of water (penalizing the net efficiency of the cycle), using CO_2 as the working fluid, the loss of exergy during the change phase can be avoided: since its critical temperature is lower (31 °C) than that of water (374 °C), the cycle is carried out without encountering the phase transition “bell”.

2. Presentation of E-Matiant and Allam Cycles

2.1. E-Matiant Cycle Layout

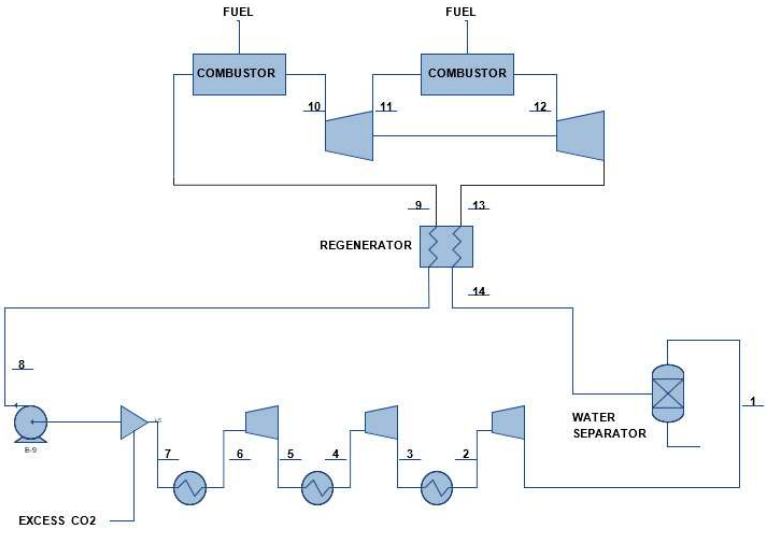

Figure 1: E-Matiant cycle layout.

It is a CO2 cycle similar to the Ericsson one with 2 quasi-isothermal processes (inter-refrigerated compression and expansion with reheating) and 2 isobaric processes (in the heat exchangers and the combustion chamber).

Starting from point 1, in atmospheric conditions, a flow of almost pure CO2 is compressed, through a three-stage intercooler compressor, up to 80 bar and 35 °C (point 7), where it is in a liquid state.

Since 80 bar is a supercritical pressure, the working fluid reaches the liquid state without entering the saturation line; this leads to two main advantages: there are no problems concerning non-condensable gases and a condenser is not necessary.

From point 7, the liquid CO_2 is compressed by a pump at the maximum cycle pressure, about 150 bar (point 8). After the pump, the fluid enters the regenerative heat exchanger, where it reaches a temperature of about 800 °C, recovering the heat of the fumes leaving the low-pressure turbine. The first combustion brings the gas to the maximum temperature of the cycle (about 1300 °C). Then the fluid expands in the high pressure (HP) turbine up to a pressure of 40 bar. In post-combustion the fluid reaches a temperature of 1300 °C again and subsequently expands in the low-pressure turbine, producing power. Then it cools by passing through the warm side of the regenerator heat exchanger (RHE), points 13-14. The water produced in the two combustion processes is almost completely separated from the CO_2 in a condensing water separator and then removed from the cycle. The excess CO_2, produced in the combustion processes, is removed in the liquid state through a valve before entering the pump (point 7).

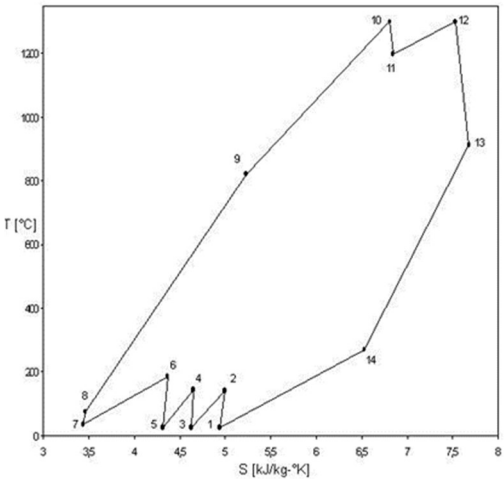

Figure 2: T-s diagram Matiant cycle [3].

2.2. Allam Cycle Layout

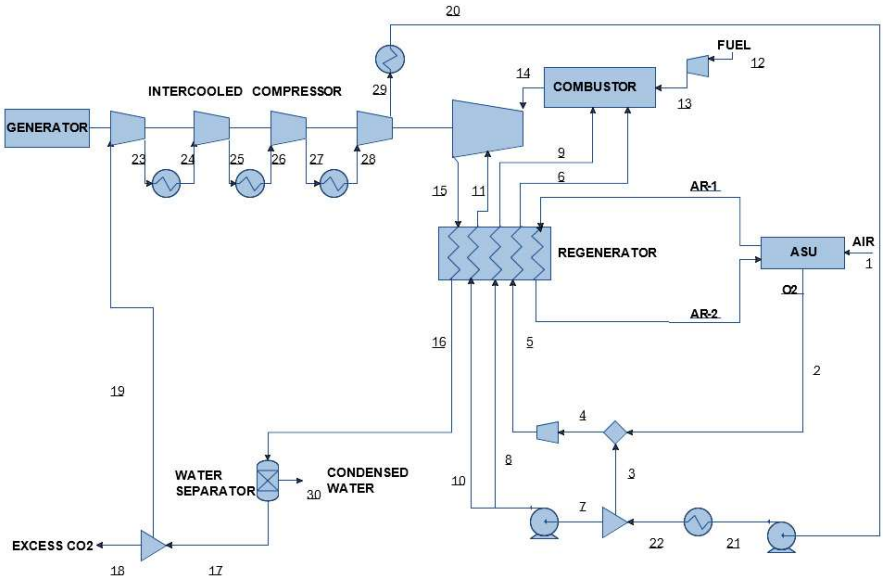

Figure 3: Allam cycle layout.

The nearly pure oxygen (99.5% purity, molar base) pressurized at 120 bar is supplied by a Cryogenic Air Separation Unit (ASU) (flow 2) and then is mixed with the CO_2 flow 3 (120 bar, 26 °C, 551 kg / s), then compressed up to the pressure of the combustor (5) (300 bar, 45 °C, 612.8 kg / s), preheated in the RHE to about 720 °C (6) and finally sent to the combustor (oxygen is mixed with CO_2 before being preheated in the regenerator for safety reasons). The combustor operates at about 300 bar and the temperature is moderate by injecting a recycling stream of CO_2 (stream 9). The hot combustion gases (14), at temperatures around 1150 °C, enter a single gas turbine that operates at high pressure and low-pressure ratio, limited between 6 and 12 [8].

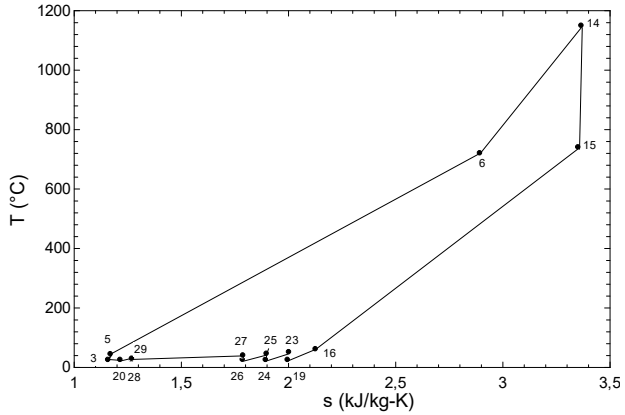

Figure 4: T-s diagram Allam cycle.

The fumes (15) at approximately 750 °C and 34 bar (1409.6 kg / s) then enter a multi-flow heat exchanger (the regenerator) which allows to efficiently recover the available heat by preheating flows 8 (300 bar, 50 °C) and 5 (45 °C, 300 bar) and the cooling flow of the turbine (flow 10). At the outlet of the regenerator, the exhaust stream (16) is cooled close to ambient temperature (17) in a chiller that condenses and separates the water (30). The remaining stream (17) is essentially pure CO_2 in the gaseous phase (T = 26 °C). Part of this stream is separated and sent to the purification, compression and storage of CO_2, while the majority (stream 19, approximately 95% of stream 17) is compressed. The intercooler compressor pressurizes the recycle flow to approximately 80 bar and the aftercooler brings it close to ambient temperature (20). Since these conditions are supercritical (dense phase CO_2) and correspond to a very high-density value of about 700 kg / m3, compression from 80 bar to the combustor pressure is performed with multistage centrifugal pumps.

A 120 bar CO_2 stream (stream 3) is extracted and mixed with pressurized O_2 supplied by the ASU. Through a compressor, it is pressurized up to 300 bar (5).

In the regenerator, the heat released by the flow at the turbine exhaust (point 15, 34 bar) is lower than that required by the high-pressure flow 5 to reach the temperature T_6 and be introduced into the combustion chamber. The cause of this difference is that the constant pressure specific heat of CO_2 increases with pressure, especially at low temperatures. Part of the heat required is provided by the condensation of the water in the turbine exhaust gases (at temperatures below 120 °C), the remainder is supplied by the ASU cooler via a heat transfer fluid circuit, in this case, it is assumed that it was air (AR-1).

2.2.1. Regenerator

It involves multiple hot and cold flows: the exhaust flow from the turbine (15), the recycled CO_2-rich flow (5), the flow that moderates the temperature in the combustion chamber (8), the cooling flow of the turbine (10) and the heat transfer fluid that transfers heat from the ASU (AR-1).

The CO_2 regenerator is considerably influenced by the change in the thermodynamic properties of the flows involved therein: by the condensation of the vapor below the dew point of flow 15 and by the different temperatures with which the hot and cold flows enter and leave the regenerator (the flows 5,8,10 enter the regenerator at temperatures of T_5=47, T_8=54 e T_{10}=54°C respectively, and leave at temperatures T_6=721, T_9=721 e T_{11}=183°C; hot flows 15 and AR-1 enter at temperatures $T_{15} = 741°C$ and $T_{AR-1} = 275°C$ and exit at the temperature

of 62 °C). The regenerator is therefore modeled as a heat exchanger between a cold composite curve and a hot composite curve, HX1 and HX2, (with variable thermal capacities).

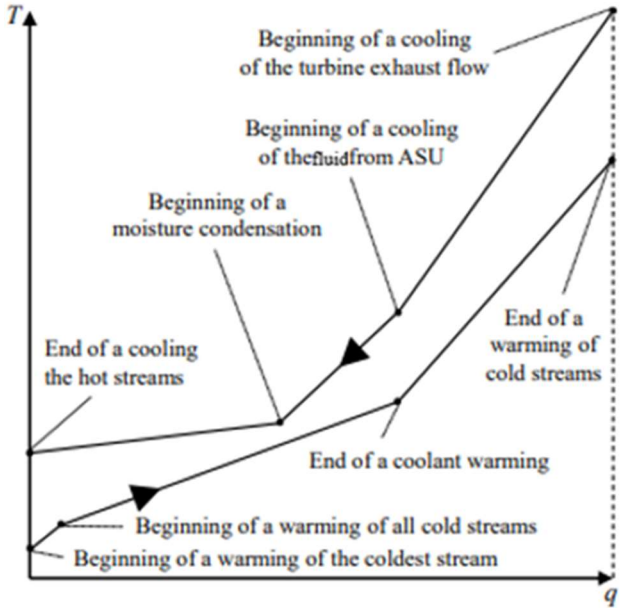

Figure 5: T-q diagram Allam cycle regenerator [9].

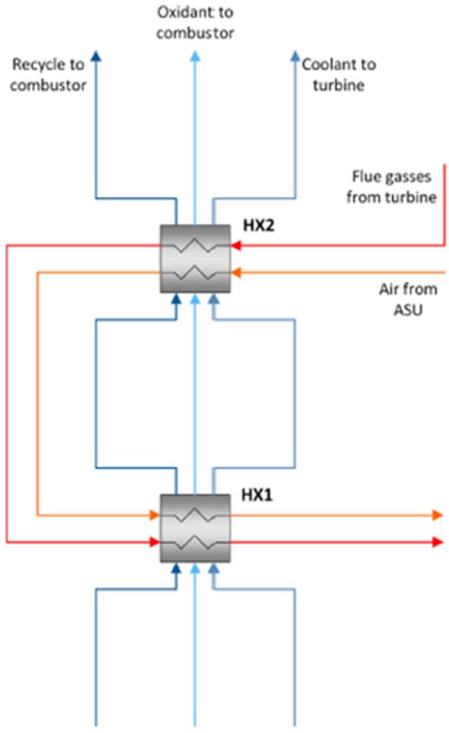

Figure 6: Flowsheet model of Allam cycle regenerator [7].

There are three possible pinch points in the regenerator, as shown in the Temperature-Enthalpy (heat output) diagram: one at the dew point of the turbine exhaust flow, a second on the hot side at the start of fluid cooling of the ASU and one third at the exit of the cold flows.

In particular, with the data assumed in this analysis, the pinch occurs at the dew temperature for hot flows and the $\Delta T_{pp} = 5°C$, while the temperature difference between the two curves on the hot side $\Delta T_{approach} = 20°C$.

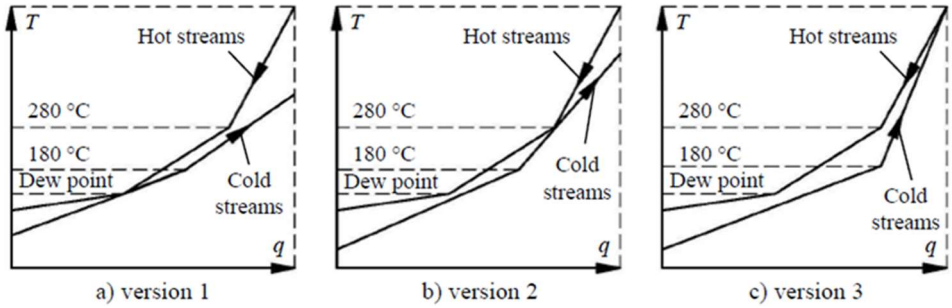

Figure 7: Regenerator T-q diagram versions [9].

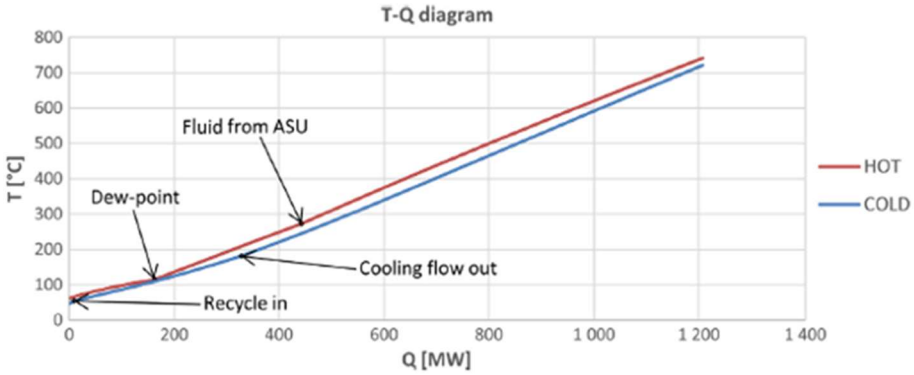

Figure 8: Possible T-Q diagram of the regenerator [7].

Thanks to the regenerator, efficient exploitation of the heat available in the fumes is possible: the outlet temperature of the flows sent to the combustor is raised, giving the cooling flow of the turbine only the remaining heat. The high temperature at the combustor inlet leads to a great advantage in terms of fuel savings. Heating the turbine cooling flow has the advantage of increasing the turbine power but also the drawback of causing an increase in turbine head losses.

2.2.2. ASU

As the purpose of this study is to focus on the Allam cycle, the detailed air separation process has not been reported, therefore the ASU is modeled as a black box.

Inside the ASU, multistage compression with interstage cooling is used. The heat released in the cooling is also used in the RHE regenerator to preheat the flow entering the combustion chamber using a heat transfer fluid (in such a way as to provide additional heat to add to the one released by the gases at the turbine exhaust).

2.3. Comparison between Allam-Matiant Cycles

Both cycles use carbon dioxide as a working fluid and pure oxygen as an oxidizer, and, since they do not release anything into the atmosphere, they can be considered zero-emission. The layouts differ because in the Matiant cycle there is the presence of reheat and therefore of high and low-pressure turbine bodies, while the Allam cycle has single combustion and a single turbine body.

Both cycles have a regenerative exchanger that preheats the flow destined for combustion, but in the Allam cycle not only the fumes coming out of the turbine and the flow directed to the combustor is involved, but also the cooling flows of the turbine (11) and of the combustor (9) and the heat transfer fluid that cools the ASU (AR-1).

Regarding the pressures, those ones in the Matiant cycle are lower, reaching the outlet of the LP turbine up to atmospheric pressure, instead of in the Allam cycle the minimum pressure is equal to 30 bar and the maximum one is 300 bar (about double that of the Matiant).

Table 1: Comparison between Allam-Matiant cycles.

Allam Cycle	E-Matiant Cycle
CO_2 working fluid	CO_2 working fluid
Pure oxygen oxidizing fluid	Pure oxygen oxidizing fluid
Zero-emission cycle	Zero-emission cycle
Layout	**Layout**
Inter-refrigerated compression (4 stages)	Inter-refrigerated compression (3 stages)
Pump	Pump
Regenerative heat exchanger	Regenerative heat exchanger
Combustion	Combustion and afterburning
Turbine	High and low pressure turbine
Condensation water separator	Condensation water separator
Removal of excess CO_2 in the gaseous phase (before intercooled compression)	Removal of excess CO_2 in the liquid phase (after intercooled compression)
Maximum cycle pressure: 300 bar	Maximum cycle pressure: 150 bar
Minimum pressure: 30-60 bar	Minimum pressure :1 bar
Efficiency: 55-59%	Efficiency: 44-45%

The efficiency of the Allam cycle is around 55-59%, the Matiant cycle is around 44-45%. Some studies have confirmed the advantages of the Allam cycle both in terms of efficiency and economy.

3. Methodology

3.1. Cycle Modeling

- The cycle analysis was carried out using the EES (Engineering Equation Solver) program.
- As regards the modeling of the cycle, the following have been assumed as known data:
  - the pressure values at each point;
  - the maximum temperature (T_{15}= 1150 °C) and minimum (T_{24}= T_{26} = T_{28}= T_{20}= T_{22}= T_{17}= 26 °C) of the cycle;
  - the temperature of the cooling air of the turbine (T_{11}= 183 °C);
  - the ΔT_{pp} and the ΔT_{app} of the regenerator (respectively equal to 5 and 20 °C);
  - the air temperature of the ASU entering the regenerative exchanger ($T_{AR,1}$);
  - the isentropic efficiencies of the compressors and turbines;
  - the mass flow rate $\dot{m}_3$, $\dot{m}_8$, $\dot{m}_{10}$.
- The fuel flow rate was obtained by imposing the energy balance in the combustor. The oxygen flow rate was obtained assuming stoichiometric combustion of the fuel.
- For the calculation of the enthalpies and entropies, the temperature T_{amb}= 25 °C and the pressure P_{amb}= 101325 Pa were taken as reference conditions, to which the standard enthalpy and entropy values of formation were then added respectively.

3.2. Assumption

The pressure losses inside the regenerator are neglected.

The ASU is considered as a component external to the cycle, therefore the power required by it has not been taken into consideration, but the heat transferred by the air inside the regenerative exchanger has been taken into account by inserting its contribution inside of efficiencies.

3.3. Turbine Modeling

In the modeling of the turbine, the presence of two incoming flows (the main flow (14) and the cooling flow (11)) and an outgoing flow (15) was considered. Since the temperatures in this part of the cycle are very high, it was assumed to consider the mixture of CO_2 and steam as perfect gases, it was, therefore, possible to apply the correlations 2 and 3.

$$T_{out,is} = T_{in}\left(\frac{P_{out}}{P_{in}}\right)^{\varepsilon} \tag{2}$$

$$T_{out} = T_{in} + \eta_{is,tur}\left(T_{out,is} - T_{in}\right) \tag{3}$$

Through these ones, having known the temperatures T_{14} and T_{11}, it was possible to obtain T_{15}.

3.4. Regenerator Modeling

The regenerator was modeled by dividing the regenerator into 4 sections, in relation to the entry/exit of the flows involved. In each section it was assumed to have flows with constant specific heats and equal to the average values of the specific heats at the inlet and outlet temperatures, however, since the purpose was to determine the temperatures at the ends of the sections, an iterative calculation was performed. On the other hand, regarding section 4, where water condensation occurs in the flow of CO_2 and steam coming out of the turbine, due to the complexity of the calculations, the Refprop program was used for the calculation of the properties of the blends.

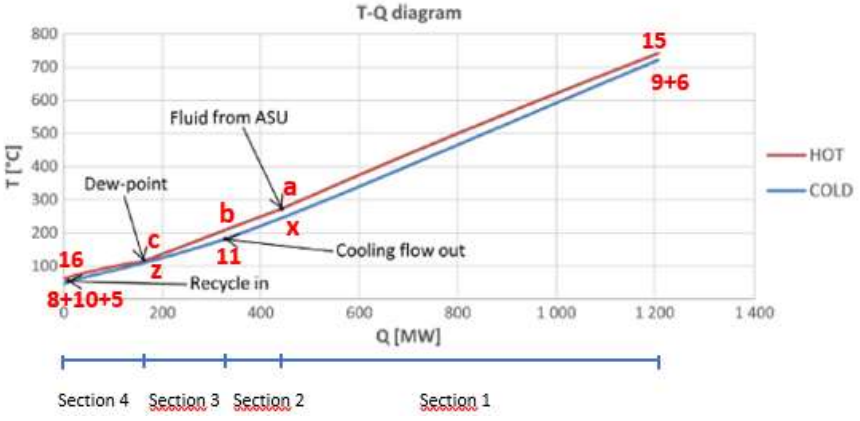

Figure 9: T-Q diagram of the regenerator.

Section 1

Table 2: Hot and cold streams of section 1 of the RHE.

Hot Streams	Turbine Exhaust Flow
Cold streams	Oxidant stream to the combustor Temperature moderating stream in the combustion chamber

Table 3: Unknown and known parameters of section 1 of the RHE.

Known Parameters	Unknown Parameters
T_{15}	T_6
T_a (inlet temperature of the air coming from the ASU)	T_9
ΔT_{app}	T_x
$\dot{m}_{hot,1} = \dot{m}_{15}$	
$\dot{m}_{cold,1} = \dot{m}_6 + \dot{m}_9$	

The solution of section 1 is carried out by applying the following equations:

$$T_9 = T_{15} - \Delta T_{app} \tag{4}$$

$$T_6 = T_{15} - \Delta T_{app} \tag{5}$$

$$cp_{hot,1} = \frac{cp_{hot,1}(T_{15}) + cp_{hot,1}(T_a)}{2} \tag{6}$$

$$cp_{cold,1} = \frac{cp_{cold,1}(T_6) + cp_{cold,1}(T_x)}{2} \tag{7}$$

$$T_x = T_6 - \frac{\dot{m}_{hot,1} \cdot cp_{hot,1} \cdot (T_{15} - T_a)}{\dot{m}_{cold,1} \cdot cp_{cold,1}} \tag{8}$$

Sections 2 and 3

Table 4: Hot and cold streams of sections 2 and 3 of the RHE.

Hot streams section 2 e 3	Turbine exhaust flow Air from ASU
Cold streams section 2	Oxidant stream to the combustor Temperature moderating stream in the combustion chamber
Cold streams section 3	Oxidant stream to the combustor Temperature moderating stream in the combustion chamber Cooling flow of the turbine

Table 5: Unknown and known parameters of sections 2 and 3 of the RHE.

Known Parameters	Unknown Parameters
T_a (inlet temperature of the air coming from the ASU)	T_z (temperature of the cold streams at pinch point)
T_c (dew temperature of the flow exiting the turbine, obtained by imposing the saturation condition on the partial pressure of the steam contained in the flow)	T_b
T_x	$\dot{m}_{AR}$ (mass flow rate of air from the ASU)
T_{11}(turbine cooling flow temperature)	
ΔT_{pp}	
$\dot{m}_{cold,2} = \dot{m}_6 + \dot{m}_9$ $\dot{m}_{cold,3} = \dot{m}_6 + \dot{m}_9 + \dot{m}_{11}$	

The solution of sections 2 and 3 is obtained as follows:

$$T_z = T_c - \Delta T_{pp} \tag{9}$$

$$cp_{cold,2} = \frac{cp_{cold,2}(T_x) + cp_{cold,2}(T_{11})}{2} \tag{10}$$

$$cp_{cold,3} = \frac{cp_{cold,3}(T_z) + cp_{cold,3}(T_{11})}{2} \tag{11}$$

$$cp_{tef,ac} = \frac{cp_{tef}(T_a) + cp_{tef}(T_c)}{2} \tag{12}$$

$$\dot{m}_{AR} = \frac{\dot{m}_{cold,2} \cdot cp_{cold,2} \cdot (T_x - T_{11}) + \dot{m}_{cold,3} \cdot cp_{cold,3} \cdot (T_{11} - T_z) - \dot{m}_{15} \cdot cp_{tef,ac} \cdot (T_a - T_c)}{cp_{air} \cdot (T_a - T_c)} \tag{13}$$

$$\dot{m}_{hot,2} = \dot{m}_{AR} + \dot{m}_{15} \tag{14}$$

$$cp_{hot,2} = \frac{cp_{tef,ac} \cdot \dot{m}_{15} + cp_{air} \cdot \dot{m}_{AR}}{\dot{m}_{hot,2}} \tag{15}$$

$$T_b = T_a - \frac{\dot{m}_{cold,2} \cdot cp_{cold,2} \cdot (T_x - T_{11})}{\dot{m}_{hot,2} \cdot cp_{hot,2}} \tag{16}$$

Section 4

Table 6: Hot and cold streams of section 4 of the RHE.

Hot streams	Turbine exhaust flow with condensation Air from ASU
Cold streams	Oxidant stream to the combustor Temperature moderating stream in the combustion chamber Cooling flow of the turbine

Table 7: Unknown and known parameters of section 4 of the RHE.

Known Parameters	Unknown Parameters
T_c	T_{16}
T_z	
$T_8 = T_{10}$	
T_5	
$\dot{m}_{hot,4} = \dot{m}_{15} + \dot{m}_{AR}$	
$\dot{m}_{cold,4} = \dot{m}_6 + \dot{m}_9 + \dot{m}_{11}$	

The resolution of section 4 is carried out by applying the following equations:

$$cp_{hot,4} = \frac{cp_{hot,4}(T_c) + cp_{hot,4}(T_{16})}{2} \tag{17}$$

$$cp_{cold,4} = \frac{cp_{cold,4}(T_z) + cp_{cold,4}(T_8)}{2} \tag{18}$$

$$T_{16} = T_c - \frac{\dot{m}_{cold,4} \cdot cp_{cold,4} \cdot (T_z - T_8)}{\dot{m}_{hot,4} \cdot cp_{hot,4}} \tag{19}$$

3.5. Combustor Modeling

The combustor was analyzed by imposing the energy balance between the fuel flow (13), the main flow of CO_2 and O_2 (6) and the temperature moderating flow (9). Since the outlet temperature was known (1150 °C) and the temperatures of flows 6 and 9 were obtained by imposing the ΔT_{app} of the regenerator (T_6= T_9=T_{15}-ΔT_{app}), the used flow rates of fuel and oxygen can be calculated.

3.6. Compressor Modeling

The compressors have been studied by imposing the compression ratio and the isentropic efficiency.

$$P_{out} = \beta \cdot P_{in} \tag{20}$$

$$h_{out} = h_{in} + \frac{1}{\eta_{is,comp}}(h_{out,is} - h_{in}) \tag{21}$$

3.7. Modeling of Heat Exchangers and Water Separator

The intercooling heat exchangers were analyzed by imposing the outlet temperature T = 26 °C and the pressure loss (equal to 2%). Instead, the analysis of the refrigerant fluid was neglected.

As regards the water separator, complete condensation of the steam produced in the combustion chamber and cooling down to a temperature of 26 °C was assumed.

3.8. Thermodynamic Analysis

Once the points of the cycle and the related enthalpies and entropies had been determined, the efficiency of the cycle was calculated, both directly and inversely.

$$\eta_{dir} = \frac{W}{Q_{ASU} + \sum m_{in}h_{in} - \sum m_{out}h_{out}} \tag{22}$$

$$\eta_{inv} = 1 - \frac{Q_c}{Q_{ASU} + \sum m_{in}h_{in} - \sum m_{out}h_{out}} \tag{23}$$

Where W is the net work of the cycle (turbine work minus that of pumps and compressors), Q_c is the heat that is transferred to the outside. The denominator is the heat supplied by the ASU and the difference between the enthalpies of the incoming flows (2 and 12) and the outgoing flows (30 and 18).

3.9. Exergetic Analysis

In the exergetic analysis, the contributions of both physical exergy and chemical exergy were taken into account using equations 24 and 25:

$$E_{ph} = \sum_i \dot{m}_i\left[h_i - h_{i,0} - T_0\left(s_i - s_{i,0}\right)\right] \tag{24}$$

$$E_{ch} = \sum_i (\dot{n}_i R_0 T_0 \ln x_i + \dot{n}_i \varepsilon_{0,i}) \tag{25}$$

Where $\varepsilon_{0,i}$ are the standard chemical exergies and x_i the molar fractions of the i-th chemical species [2].

First, the exergy of each point of the cycle was calculated. Subsequently, the exergetic losses/destruction for each component of the cycle were calculated, finally, the yield of the second principle, both direct and inverse, was calculated, verifying their equality.

$$\eta_{ex,dir} = \frac{W}{Q_{ASU} + \sum E_{in}} \tag{26}$$

$$\eta_{ex,inv} = 1 - \frac{\sum(Ed_i + El_i)}{Q_{ASU} + \sum E_{in}} \quad (27)$$

Where W is the net work of the cycle (turbine work minus that of pumps and compressors), Ed_i and El_i are and destruction and exergy losses (including E_{18} and E_{30}). In the denominator we have the exergies of the incoming flows (12 and 2) and the heat provided by the ASU.

4. Results

The results shown in Table **8** are deduced from the analysis of the cycle.

Table 8: Thermodinamic and exergetic analysis resutsresult.

	m[i] [kg/s]	p[i] [Pa]	T[i] [°C]	h[i] [J/(kg)]	s[i] [J/(kg*K)]	s0[i] [J/(kg*K)]	h0[i] [J/(kg)]	ex[i] [J/kg]	ext[i] [W]
1	Air entering the ASU								
2	61,49	1,20E+07	15	-39351	-1356,13	-0,00	0,005425	480623	2,96E+07
3	551,10	1,20E+07	26	-9,19E+06	3274,19	4852,80	-8,94E+06	671190	3,70E+08
4	612,59	1,20E+07	23,69	-8,27E+06	2868,77	4442,90	-8,04E+06	634332	3,89E+08
5	612,59	3,00E+07	51,12	-8,23E+06	2923,08	4442,90	-8,04E+06	659818	4,04E+08
6	612,59	3,00E+07	717,8	-7,31E+06	4553,86	4442,90	-8,04E+06	1,10E+06	6,71E+08
7	741,30	1,20E+07	26	-9,19E+06	3274,19	4852,80	-8,94E+06	671190	4,98E+08
8	641,90	3,00E+07	49,71	-9,16E+06	3317,32	4852,80	-8,94E+06	692765	4,45E+08
9	641,90	3,00E+07	717,8	-8,21E+06	5006,08	4852,80	-8,94E+06	1,14E+06	7,34E+08
10	99,40	3,00E+07	49,71	-9,16E+06	3317,32	4852,80	-8,94E+06	692765	6,89E+07
11	99,40	3,00E+07	183	-8,90E+06	3981,32	4852,80	-8,94E+06	749159	7,45E+07
12	15,41	7,00E+06	15	-4,67E+06	9338,57	11609,45	-4,65E+06	5,25E+07	8,09E+08
13	15,41	3,00E+07	133	-4,39E+06	9401,10	11609,46	-4,65E+06	5,28E+07	8,13E+08
14	1269,90	3,00E+07	1150	-7,73E+06	5681,61	4873,10	-9,13E+06	1,60E+06	2,04E+09
15	1369,30	3,30E+06	737,8	-8,27E+06	5661,00	4872,50	-9,12E+06	1,06E+06	1,45E+09
16	1369,30	3,30E+06	60,68	-9,10E+06	4259,50	4872,50	-9,12E+06	637985	8,74E+08
17	1334,68	3,30E+06	26	-8,98E+06	4112,16	4852,80	-8,94E+06	638129	8,52E+08
18	42,28	3,30E+06	26	-8,98E+06	4112,16	4852,80	-8,94E+06	638129	2,70E+07
19	1292,40	3,30E+06	26	-8,98E+06	4112,16	4852,80	-8,94E+06	638129	8,25E+08
20	1292,40	8,00E+06	26	-9,18E+06	3330,36	4852,80	-8,94E+06	666284	8,61E+08
21	1292,40	1,22E+07	33,43	-9,17E+06	3338,40	4852,80	-8,94E+06	671790	8,68E+08
22	1292,40	1,20E+07	26	-9,19E+06	3274,19	4852,80	-8,94E+06	671190	8,67E+08
23	1292,40	4,55E+06	51,9	-8,96E+06	4117,41	4852,80	-8,94E+06	653595	8,45E+08
24	1292,40	4,46E+06	26	-8,99E+06	4009,74	4852,80	-8,94E+06	651243	8,42E+08
25	1292,40	5,79E+06	46,81	-8,98E+06	4013,57	4852,80	-8,94E+06	662340	8,56E+08
26	1292,40	5,67E+06	26	-9,02E+06	3895,22	4852,80	-8,94E+06	660299	8,53E+08
27	1292,40	6,82E+06	40,1	-9,01E+06	3897,53	4852,80	-8,94E+06	666846	8,62E+08
28	1292,40	6,58E+06	26	-9,06E+06	3751,26	4852,80	-8,94E+06	664775	8,59E+08
29	1292,40	8,16E+06	40,16	-9,05E+06	3753,29	4852,80	-8,94E+06	670514	8,67E+08
30	34,62		26	-1,60E+07	3896,07	3882,93	-1,59E+07	422722	1,46E+07

The parameter of the air entering the ASU is not specified as this component is considered external to the Allam cycle.

The values obtained from this analysis were compared with those achieved by Scaccabarozzi *et al*. [7] and by Mancuso *et al*. [4]; from this comparison, it can be seen that the results of the investigations agree with each other as the variations in the values of the main thermodynamic parameters are contained.

From the exergetic analysis for each component, the destruction/losses shown in Table 9 are obtained. In the column on the right, the values divided by the incoming exergy are shown.

Table 9: Exergetic losses / destructions in Allam cycle components.

	Component$[i]	Ed[i] [W]	Ed_r[i]
1	1^{st} compressor	2,02E+06	0,002259
2	2^{nd} compressor	1,48E+06	0,001648
3	3^{rd} compressor	890674	0,0009944
4	4^{th} compressor	780247	0,0008711
5	5^{th} compressor	9,92E+06	0,01107
6	2^{nd} pump	3,10E+06	0,00346
7	1^{st} pump	9,53E+06	0,01064
8	CH_4 compressor	287358	0,0003208
9	turbine	4,20E+07	0,04686
10	1^{st} intercooler	3,04E+06	0,003395
11	2^{nd}intercooler	2,64E+06	0,002945
12	3^{rd} intercooler	2,68E+06	0,002988
13	4^{th} intercooler	5,47E+06	0,006104
14	5^{th} intercooler	775761	0,0008661
15	water condensator	7,26E+06	0,008104
16	mixer of flows 2 and 3	1,09E+07	0,01213
17	splitter of flows 3 and 7	0	0
18	splitter of flows 18 and 19	0	0
19	CO_2 removal	2,70E+07	0,03012
20	H_2O removal	1,46E+07	0,01634
21	regenerator	6,86E+07	0,07654
22	combustor	1,83E+08	0,2048
23	splitter of flows 8 and 10	0	0

The results show that the greatest exergetic losses / destructions occur in the combustor (about 20% of the incoming exergy) and in the regenerator (about 7,6%). Therefore, these two components are the ones on which the most attention must be paid.

From the thermodynamic analysis of the cycle, it can be concluded that the net power of the cycle is W=499.4 MW.

In addition, a first principle efficiency is obtained in line with expectations: η = 0.5459.

From the exergetic analysis, a second principle efficiency η_{ex} = 0.5575 was obtained.

These values are interesting because they show that with this type of technology it is possible to create plants that, in addition to being zero-emission ones, have good efficiencies when compared to those of conventional plants. Further studies in this area and the creation of prototypes are therefore encouraged so that these plants can be used for energy production in the near future.

5. Conclusions

In this study, research on the Allam cycle was conducted. It started with the presentation of the reasons for the implementation of cycles with oxy-combustion having carbon dioxide as a working fluid, such as the reduction of emissions into the atmosphere and the greenhouse effect. A comparison was then made between the layouts of the Matiant and Allam cycles, showing similarities and differences in the management of flows and the pressures involved. Finally, the thermodynamic and exergetic analysis of the cycle was carried out following the modeling criteria reported in paragraph 3. The values of the thermodynamic parameters obtained are in agreement with those reported in other studies and it leads us to think the analysis and the assumptions made are correct. However, the model developed requires further improvements, in particular, it would be good for a turbine cooled in stages, rather than in a point-like way, and to carry out a parametric analysis of the main thermodynamic quantities in order to achieve an optimization of the cycle.

The calculated thermodynamic efficiency confirms the advantages deriving from this cycle and therefore the interest in this area. From the exergetic analysis, it is clear that the main components in which exergetic destruction/losses occur are combustor and regenerator and for this reason, they are the components whose management must be subjected to particular attention.

Nomenclature

ASU	Air Separation Unit
cp_{air}	Constant pressure specific heat of air from the ASU, $\frac{J}{kg\ K}$
$cp_{cold,i}$	Constant pressure specific heat of cold streams in the i-th section of RHE, $\frac{J}{kg\ K}$
$cp_{hot,i}$	Constant pressure specific heat of hot streams in the i-th section of RHE, $\frac{J}{kg\ K}$
cp_i	Constant pressure specific heat, $\frac{J}{kg\ K}$
cp_{tef}	Constant pressure specific heat of turbine exhaust flow $\frac{J}{kg\ K}$
E_{ch}	Chemical exergy, W
Ed_i	Exergy destruction, W
E_i	Exergy, W
E_{in}	Inlet exergy, W
El_i	Exergy losses, W
E_{ph}	Physical exergy
$h_{i,0}$	Enthalpy in reference conditions, $\frac{J}{kg}$
h_{in}	Inlet enthalpy, $\frac{J}{kg}$
$h_{out,is}$	Outlet enthalpy in isoentropic conditions, $\frac{J}{kg}$
h_{out}	Outlet enthalpy, $\frac{J}{kg}$
$\dot{m}_i$	Mass flow rate, $\frac{kg}{s}$
$\dot{m}_{cold,i}$	Mass flow rate of cold streams in the i-th section of RHE, $\frac{kg}{s}$
$\dot{m}_{hot,i}$	Mass flow rate of hot streams in the i-th section of RHE, $\frac{kg}{s}$
$\dot{n}_i$	Molar flow rate, $\frac{kmol}{s}$

P_{amb}	Ambient pressure, Pa
P_i	Pressure, Pa
P_{in}	Inlet pressure, Pa
P_{out}	Outlet pressure, Pa
Q_{ASU}	ASU thermal power
RHE	Regenerator heat exchanger
R_0	Universal gas constant, $\frac{J}{kmol\ K}$
$s_{i,0}$	Entropy in reference conditions, $\frac{J}{kg\ K}$
s_i	Entropy, $\frac{J}{kg\ K}$
T_0	Reference temperature, °C
T_{amb}	Ambient temperature, °C
T_i	Temperature, °C
$T_{out,is}$	Temperature in isoentropic conditions, °C
W	Net power output
x_i	Molar fraction
β	Pressure ratio
ΔT_{app}	Regenerator hot side ΔT
ΔT_{pp}	Regenerator pinch point ΔT
ε	Exponent isentropic transformations
$\varepsilon_{0,i}$	Standard chemical exergy, $\frac{J}{kmol}$
η	Efficiency
η_{dir}	Direct efficiency
$\eta_{ex,dir}$	Direct exergetic efficiency
$\eta_{ex,inv}$	Indirect exergetic efficiency
η_{ex}	Exergetic efficiency
η_{inv}	Indirect efficiency
$\eta_{is,comp}$	Compressor isoentropic efficiency
$\eta_{is,tur}$	Turbine isoentropic efficiency

References

[1] Fernandes D, Wang S, Xu Q, Buss R, Chen D. Process and carbon footprint analyses of the Allam cycle power plant integrated with an air separation unit. Clean Technologies, 2019. https://doi.org/10.3390/cleantechnol1010022

[2] Guohui, Jun S, Hao X, Laihong Z, Shen. A unified correlation for estimating specific chemical exergy of solid and liquid fuels; Energy 2012; 40: 164-173. https://doi.org/10.1016/j.energy.2012.02.016

[3] Lombardi L. Life cycle assessment comparison of technical solutions for CO2 emissions reduction in power generation; Energy Conversion and Management 2003; 44: 93-108. https://doi.org/10.1016/S0196-8904(02)00049-3

[4] Mancuso L, Ferrari N, Chiesa P, Martelli E, Romano MC. Oxy-combustion turbine power plants. IEAGHG report 2015/05, August, 2015.

[5] Diego ME, Finney KN, Pourkashanian M. The Sustainable Option of Power from Fossil Fuels with Carbon Capture and Storage: An Overview of State-of-the-Art Technology; Sustainable Energy Technology and Policies pp 195-229. https://doi.org/10.1007/978-981-10-7188-1_9

[6] Mathieu P, Dubuisson R, Houyou S, Nihart R. New concept of co2 removal technologies in power generation, combined with fossil fuel recovery and long term co2 sequestration; Proceedings of the ASME TURBO EXPO 2000 May 8-11, 2000 - Munich, Germany. https://doi.org/10.1115/2000-GT-0160

[7] Scaccabarozzi R, Gatti M, Martelli E. Thermodynamic analysis and numerical optimization of the NET Power oxy-combustion cycle; Applied Energy 2016; 178: 505-526. https://doi.org/10.1016/j.apenergy.2016.06.060

[8] Allam R, Martin S, Forrest B, Fetvedt J, Lu X, Freed D, *et al*. Demonstration of the Allam Cycle: An update on the development status of a high efficiency supercritical carbon dioxide power process employing full carbon capture; 13th International Conference on Greenhouse Gas Control Technologies, GHGT-13, 14-18 November 2016, Lausanne, Switzerland; Energy Procedia 2017; 114: 5948-5966. https://doi.org/10.1016/j.egypro.2017.03.1731

[9] Rogalev V, Kindra S, Osipov N. Rogale 2, thermodynamic analysis of the net power oxy-combustion cycle, Proceedings of 13-th European Conference on Turbomachinery Fluid dynamics & Thermodynamics ETC13, April 8-12, 2018; Lausanne, Switzerland. https://doi.org/10.29008/ETC2019-030